

See discussions, stats, and author profiles for this publication at: <https://www.researchgate.net/publication/51425961>

Salt Crystallization during Evaporation: Impact of Interfacial Properties

ARTICLE *in* LANGMUIR · AUGUST 2008

Impact Factor: 4.46 · DOI: 10.1021/la8005629 · Source: PubMed

CITATIONS

52

READS

321

4 AUTHORS, INCLUDING:



Salima Rafai

French National Centre for Scientific Resea...

29 PUBLICATIONS 619 CITATIONS

SEE PROFILE



Daniel Bonn

University of Amsterdam

255 PUBLICATIONS 7,137 CITATIONS

SEE PROFILE

Salt Crystallization during Evaporation: Impact of Interfacial Properties

Noushine Shahidzadeh-Bonn,^{*,†,‡} Salima Rafai,[†] Daniel Bonn,^{†,§} and Gerard Wegdam[†]

Van der Waals-Zeeman Instituut (WZI), Universiteit van Amsterdam, Valckenierstraat 65, 1018 XE Amsterdam, The Netherlands, UR Navier, LMSGC, Université Paris-Est, 2 allée Kepler, 77420 Champs-sur-Marne, France, and Laboratoire de Physique Statistique de l'ENS, 24 rue Lhomond, 75231 Paris cedex 05, France

Received March 4, 2008. Revised Manuscript Received June 3, 2008

Salt damage in stone results in part from crystallization of salts during drying. We study the evaporation of aqueous salt solutions and the crystallization growth for sodium sulfate and sodium chloride in model situations: evaporating droplets and evaporation from square capillaries. The results show that the interfacial properties are of key importance for where and how the crystals form. The consequences for the different forms of salt crystallization observed in practice are discussed.

Introduction

Porous materials (such as stones or masonry materials) are often observed to deteriorate under environmental conditions. An important part of this damage is believed to be due to salt crystallization in the materials. Salts can be naturally present in the stones or get trapped inside the porous material, for instance, by imbibition with salt-containing precipitation (e.g., acid rain). Used as building materials, most stones will be subject to wetting and drying cycles; during the latter salts initially dissolved in water may crystallize, and the crystallization, in turn, may damage the material. Indeed, most salts are reported to cause damage when such repeated cycles of crystallization/dissolution take place, because of the impact of such cycles on the ion concentration (formation of supersaturated solutions^{1,2}) and on the structure of the precipitated salt.^{2–7} In addition, the damage also depends on the pore size distribution in the stone.^{4,6} The detailed mechanisms of the damaging processes have been investigated for several decades now. Different theoretical explanations have been proposed; the most popular ones these days are the crystallization pressure against the pore walls (which is proportional to the degree of supersaturation) and volume variations in the salt structure during wetting and drying cycles.^{5–10} However, neither of these can successfully explain why, under identical experimental conditions, certain salts such as sodium sulfate cause more damage than other high-solubility salts such as sodium chloride. For the specific case of sodium sulfate, two crystalline phases exist, and it is not yet clear which phase, hydrated or

anhydrous, is the one responsible for the damage. Consequently, a detailed understanding of how crystal growth within the porous media leads to the damage still remains elusive. What is clear is that some salts preferably crystallize on the exterior wall of the stones, a phenomenon called efflorescence, whereas others prefer to crystallize within the porous medium, called subflorescence. The latter is far more damaging than the former. We investigate here whether the interfacial properties of the salts are responsible for this, in addition to a possible dependence on the properties of salt solutions.¹¹

When subflorescence occurs, some authors presume the existence of a thin liquid film of salt solution between the salt crystal and the pore wall which allows the crystal to grow while pushing against the wall at the same time.⁶ Although this could be an explanation for the damage caused by the crystallization, there is no experimental evidence so far that this film exists. Others have argued that, because a substantial energy is normally required to produce a direct contact between the salt and stone, there is an upper bound to the crystallization pressure (which again might cause the damage) that is due to interfacial properties. Recently, Coussy⁴ argued that the difference in liquid–vapor surface tension, γ_{lv} , between sodium sulfate and sodium chloride leads to a difference in the capillary pressure gradient, which could be responsible for the very different types of damage caused by the crystallization of these two salts. The importance of the crystallization pattern of different salts such as sodium chloride and sodium sulfate as well as the importance of the location of crystallization for the damage has already been studied by Rodriguez-Navarro and Doehne.¹⁰ However, in spite of its known importance for crystal growth, up till now, the influence of the surface and interfacial properties (solid (porous matrix)–liquid and crystal–liquid) as well as wetting films in the place where crystallization appears has not been studied in any detail.

In this study we try to establish the difference between the two salts (sodium sulfate and chloride) with respect to the crystallization in model situations where one can directly assess the influence of the interfacial properties on the way crystallization takes place. We focus on microscale experiments using direct imaging and optical microscopy. The growth of salt crystallization patterns is followed during evaporation at constant relative

* To whom correspondence should be addressed. E-mail: nshahidz@science.uva.nl.

[†] Universiteit van Amsterdam.

[‡] Université Paris-Est.

[§] Laboratoire de Physique Statistique de l'ENS.

(1) Goudies, A. S.; Viles, H. A. *Salt Weathering Hazard*; Wiley: London, 1997.

(2) Flatt, R. J. J. *Cryst. Growth* **2002**, 242, 435–454.

(3) Tsui, N.; Flatt, R.; Scherer, G. W. *J. Cult. Herit.* **2003**, 4, 109–115.

(4) Coussy, O. *J. Mech. Phys. Solids* **2006**, 54, 1517–1547.

(5) Rodriguez-Navarro, C.; Doehne, E.; Sebastian, E. *Cem. Concr. Res.* **2000**, 30, 1527–1534.

(6) Scherer, G. W. *Cem. Concr. Res.* **2004**, 34, 1613–1624.

(7) Lubelli, B.; Van Hees, R. R. J.; Groot, C. J. W. P. *Stud. Conserv.* **2006**, 51, 41–56.

(8) Steiger, M. J. *Cryst. Growth* **2005**, 282, 455–469.

(9) Steiger, M. J. *Cryst. Growth* **2005**, 282, 470–481.

(10) Rodriguez-Navarro, C.; Doehne, E. *Earth Surf. Processes Landforms* **1999**, 24, 191–209.

(11) Ruiz-Agudo, E.; Mees, F.; Jacobs, P.; Rodriguez-Navarro, C. *Environ. Geol.* **2007**, 52, 269–281.

humidity and temperature on flat surfaces with well-controlled wetting properties and in square capillary tubes as simple model systems for a single pore within a porous medium. To our knowledge, the growth of a salt crystallization pattern in angular (square) capillaries has not been studied experimentally, although the latter due to the presence of wetting films represents more realistically the porous materials. We find that, depending on the type of salt used and the experimental conditions, salt crystals form either at the interface of the substrate with the salt solution or at the solution–air interface. This information is crucial to answer the question of whether a given salt will show subflorescence or efflorescence and how its crystallization causes the damage.

Experimental Section

Sodium sulfate at room temperature has two stable crystal phases: an anhydrous phase (Na_2SO_4 , thenardite) and a decahydrated phase ($\text{Na}_2\text{SO}_4 \cdot 10\text{H}_2\text{O}$, mirabilite). In addition, a metastable heptahydrated phase has been reported in some laboratory experiments.^{12,13} Mirabilite is the thermodynamically stable state in contact with a saturated solution of sodium sulfate. The stability of the hydrated/anhydrous phase in open air depends on the temperature and relative humidity. X-ray crystallography experiments on our samples show that, even if hydrated crystals are formed initially, if left in contact with air ($38 \pm 4\%$, $21 \pm 0.5^\circ\text{C}$) they will transform into an anhydrous phase (thenardite). Therefore, in contact with (dry enough) air, thenardite is the thermodynamically stable state.

The existence of several crystal structures gives the salt unusual solubility characteristics; unfortunately, in most of the papers,^{3,6,10,13} details about the solutions used in the laboratory experiments are not reported (i.e., the preparation procedure, the conductivity of the solutions, or at which moment the solution was used (freshly prepared or aged solution) to impregnate the stones, for example).

Here, the dissolution is followed by a measurement of the conductivity σ of the solution, which is proportional to the ion concentration $\sigma = \sum \lambda_i C_i$, where λ is the specific conductivity of each ion and C its concentration. The conductivity was measured using a commercially available conductimeter (Syberscan 500), which was calibrated with standard solutions of potassium chloride of known conductivity provided by Oakton. The conductivity of the calibration solutions is given as a function of temperature. The whole laboratory is thermostated at $21 \pm 0.5^\circ\text{C}$. Sodium sulfate solutions were prepared by dissolving thenardite (Sigma-Aldrich grade) little by little in distilled water ($\sigma = 0.42 \mu\text{S/cm}$) until a value of the conductivity $\sigma = 108 \text{ mS/cm}$ (18.6 wt % or 1.6 M) was reached; beyond this concentration the solution becomes turbid due to the formation of mirabilite crystals from the solution. Subsequently, the conductivity of the prepared solution is followed with time. The results show that, despite its transparent aspect, the solution evolves in time with a roughly exponential decrease of the conductivity due to the precipitation of mirabilite (hydrated crystals) (Figure 1). After one day a stable value $\sigma \approx 95 \text{ mS/cm}$ is found, which corresponds to a saturated mirabilite solution, in agreement with the reported literature value (maximum solubility of about 16.5 wt % or 1.4 M). Thus, the sulfate solution with a conductivity $\sigma = 108 \text{ mS/cm}$ at a concentration of 18.6 wt % is supersaturated with respect to the formation of mirabilite crystals ($S = C/C_s = 1.12$, where S is the supersaturation, C the existing solute concentration, and C_s the saturation concentration).

Saturated sodium chloride solutions (26.4 wt % or 6.1 M) are prepared with NaCl (Sigma-Aldrich grade). Sodium chloride is known to form cubic anhydrous crystals. The given salt concentrations are obtained from the initial drop weight, weighing the amount of salt at the end of evaporation of salt solution droplets, and averaging over more than 20 droplets.

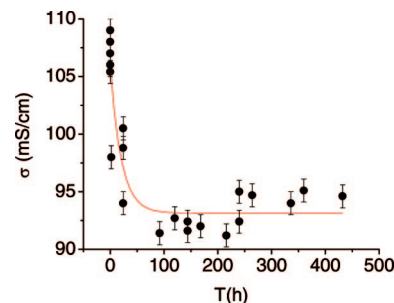


Figure 1. Evolution of the conductivity of the Na_2SO_4 solution (18.6 wt % or 1.6 M): exponential decrease, $y = A_1 \exp((-x/t_1)) + y_0$. The solution is transparent at time t_0 .

The evaporation of droplets is done in a conditioned environment with $T = 21^\circ\text{C}$ and at relative humidity $\text{RH} = 38 \pm 4\%$. On the one hand, the weight of a deposited droplet (typically $50 \mu\text{L}$) was followed in time on an automated balance with a precision of $\pm 0.001 \text{ g}$, and on the other hand, using direct imaging the formation of crystals during the evaporation was imaged. The direct imaging experiment allows us to assess which crystal forms by looking at the crystal shape and crystallization pattern.

The evaporation of droplets of the different solutions was studied on glass slides (Corning) having different wetting properties. The glass slides (standard microscope slides) are rather hydrophilic, but do not show a zero contact angle for pure water. To get a complete wetting surface ($\theta \approx 0^\circ$, for water), the slides were cleaned with sulfochromic acid and used within 2 h of cleaning. Hydrophobic surfaces were obtained by a solvent-based silanization reaction of the same glass slides using a (fluoroalkyl)silane solution (Degussa F-8261).¹⁴

The surface tensions of the different solutions ($\gamma_{\text{water}} \approx 71.7 \text{ mN/m}$, $\gamma_{\text{Na}_2\text{SO}_4} \approx 81 \text{ mN/m}$ (for $\sigma \approx 108 \text{ mS/cm}$), $\gamma_{\text{NaCl}} \approx 84 \text{ mN/m}$) were measured using the drop weight technique.¹⁵ This is a widely used standard method that relies on a force balance at the moment a droplet breaks off from a capillary of known size. The force balance is that between the gravitational force on one hand and the restoring surface tension force on the other hand. Subsequently, a small phenomenological correction factor is used that accounts for the small amount of liquid that remains attached to the capillary. This leads to a variation of the surface tension with salt concentration, that is, $\gamma = \gamma_{\text{water}}(1 + 0.0235[\text{NaCl}])$ and $\gamma = \gamma_{\text{water}}(1 + 0.0544[\text{Na}_2\text{SO}_4])$, where the concentrations are in molar units.¹⁶

Results

Droplet Evaporation. When a Na_2SO_4 droplet with conductivity $\sigma = 108 \text{ mS/cm}$ is deposited on a hydrophilic glass slide, the crystallization process starts very rapidly at the surface of the drop (the liquid–air interface) and no crystallization is observed near the contact line or in the bulk solution. Both long and short prismatic (tabular) crystals are observed, pointing to the formation of hydrated crystals. In the following, since we do not have any conclusive evidence for it, we do not discuss the nature of the hydrated phase, which may be either hepta- or decahydrated. The spontaneous formation of this crystalline phase could be due to the fact that hydrated microcrystals are likely to already be present in the solution (in spite of the clear aspect) and the evaporation results in their immediate growth. The formation of these hydrated crystals at the liquid–air interface decreases the interfacial tension γ_{lv} (otherwise the crystals would not adsorb there), leading to a rapid spreading of the droplet in time (Figure 2a) and subsequently the crystallization in the

(12) Rijmers, L. A.; Huinink, H. P.; Pel, L.; Kopinga, K. *Phys. Rev. Lett.* **2005**, *94*, 75503.

(13) Rijmers, L. A.; Pel, L.; Huinink, H. P.; Kopinga, K. *Magn. Reson. Imaging* **2005**, *23*, 273–276.

(14) Brozka, J. B.; Shahidzadeh, N.; Rondelez, F. *Nature* **1992**, *360*, 31.

(15) Campbell, J. J. *Phys. D* **1970**, *3*, 1499–1504.

(16) Weast, R. C. *Handbook of Chemistry and Physics*; CRC Press: Boca Raton, FL, 1980.

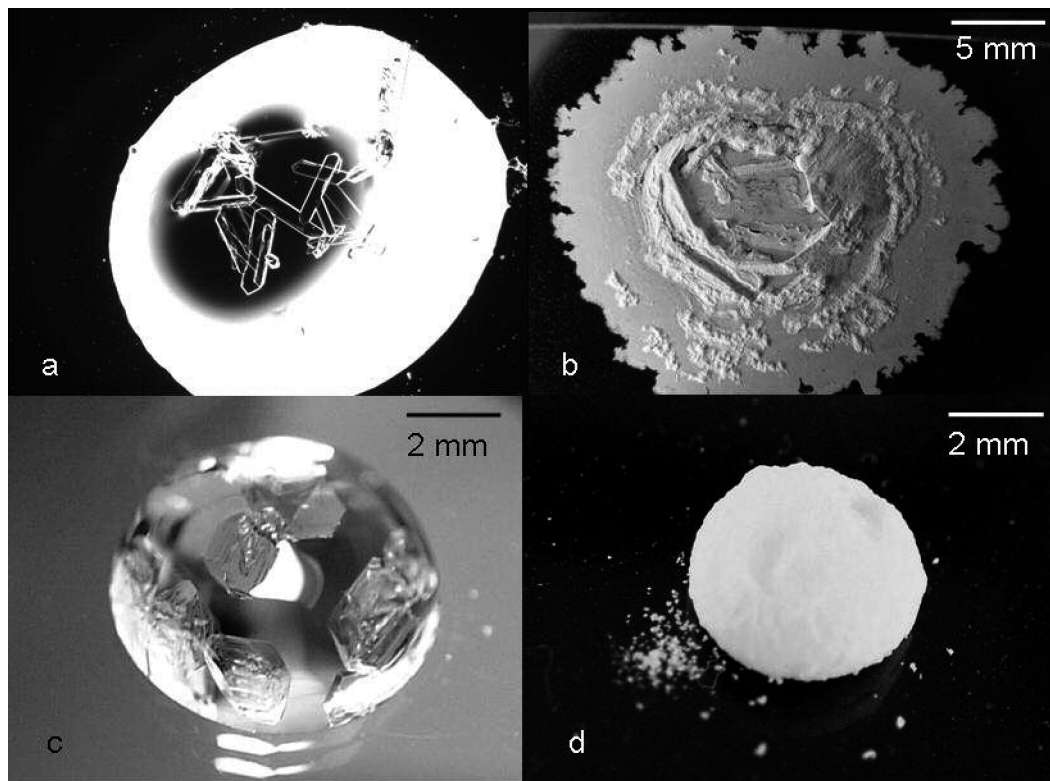


Figure 2. Salt crystallization during evaporation of supersaturated Na_2SO_4 droplets ($S \approx 1.1$, $\sigma = 108$ mS/cm). Hydrophilic surface: (a) growth of hydrated crystals at the liquid–air interface, (b) at the end of drying (the spreading film is clearly visible). Hydrophobic surface: (c) hydrated crystals at the liquid–air interface, (d) ping-pong ball shape at the end of drying.

spreading film. At the end of the drying cycle, the hydrated crystals lose their water and are transformed into the anhydrous form with a distinct white color. This allows the spreading of the film around the droplet to be clearly observed at the end of the evaporation (Figure 2b).

The spreading coefficient S is defined as the difference between the surface energies of the dry and wet solid substrates:¹⁷

$$S = E_{\text{dry}}^{\text{substrate}} - E_{\text{wet}}^{\text{substrate}} \\ S = \gamma_{\text{sv}} - (\gamma_{\text{sl}} + \gamma_{\text{lv}}) \quad (1)$$

E is the surface free energy for a given situation, determined by the different surface tensions (γ_{sv} , γ_{sl} , γ_{lv}). Now if $S < 0$, the free energy of a “dry” surface is lower than that of a “wet” surface, and thus, a droplet will not spread. At the point where S becomes zero, it becomes energetically favorable for the droplet to spread, and it will attempt to do so until the surface is completely covered. As we will see below, it turns out that the formation of hydrated crystals at the liquid–vapor interface lowers the surface tension of that same interface. This, in turn, leads to the spreading of the droplet in the experiments.

The contact angle is determined by the three interfacial tensions (liquid–vapor, solid–liquid, and solid–vapor). Zisman¹⁸ proposed that the solid–liquid interfacial tension should be independent of the liquid used. The solid–vapor interfacial tension is also usually taken to be independent of the type of liquid. In this case, the contact angle is solely determined by the liquid–vapor tension. This is generally very well verified in experiment.^{18,19} Thus, for a given substrate, it is very plausible

that the contact angle changes due to a variation in the liquid–vapor interfacial tension only. It follows from Young’s equation that

$$\gamma_{\text{lv}} \cos \theta = \gamma_{\text{sv}} - \gamma_{\text{sl}} \\ \gamma_{\text{lv}} \cos \theta = \gamma_{\text{c}} \quad (2)$$

Then, knowing the surface tension of the salt solution ($\gamma_{\text{lv}} \approx 81$ mN/m for the supersaturated Na_2SO_4 solution) and its contact angle ($\theta = 33 \pm 2^\circ$, measured in the laboratory using an image processing system) with a hydrophilic surface, we can calculate the critical surface tension.

For the hydrophilic glass slide γ_{c} is about ~ 71 mN/m. Consequently, we arrive at the conclusion that the formation of hydrated crystals at the liquid–air interface decreases the liquid–vapor interfacial tension from 81 mN/m to a value at or below 71 mN/m, leading to its complete spreading observed in the experiments. The lowering of the surface tension by the absorption of crystallites is therefore quite a sizable effect. It turns out to be very difficult to determine the changes in the liquid–vapor tension due to the appearance of crystals using the drop weight method used here to determine the liquid–vapor surface tensions. However, we did perform experiments where we deposit a new droplet right beside a dried one and observe a similar behavior for the drying of the droplet, showing that the solid–vapor surface tension does not change in the vicinity of the droplet. Therefore, the observed change must indeed come from the change in the liquid–vapor surface tension.

The same experiment using a hydrophobic surface shows again the formation of hydrated crystals at the liquid–air interface (Figure 2c). Now, due to the hydrophobic character of the solid surface, the spreading step cannot take place. Consequently, the crystals at the liquid–air interface grow and form a “skin”, keeping

(17) de Gennes, P. G.; Brochard-Wyart, F.; Quéré, D. *Gouttes, Bulles, Perles et Ondes*; Belin: Paris, 2002.

(18) Fox, H. W.; Zisman, W. A. *J. Colloid Sci.* **1950**, *5*, 514.

(19) Sghaier, N.; Prat, M.; Ben Nasrallah, S. *Chem. Eng. J.* **2006**, *122*, 47–53.

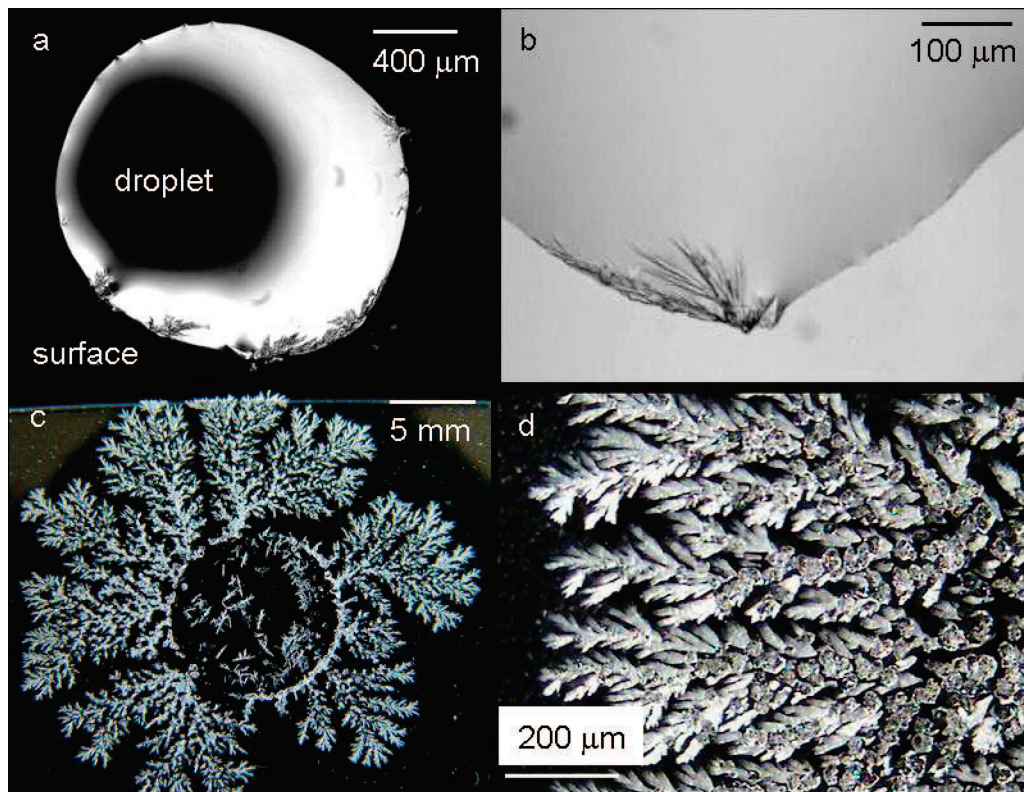


Figure 3. Salt crystallization during evaporation of saturated Na_2SO_4 droplets ($S \approx 1$, $\sigma = 95$ mS/cm) on a hydrophilic surface: (a) growth of anhydrous crystals (thenardite) at the contact line, (b) high magnification of the contact line, (c) at the end of drying (formation of dendritic anhydrous crystals due to a mesoscopic wetting film around the contact line), (d) close-up of thenardite dendritic growth.

the 3D shape of the droplet till the end of the crystallization process. At the end of the drying the crystallization has the shape of a “ping-pong” ball (Figure 2d). The silanization of the glass slide leads to a low surface energy with a critical surface tension of about $\gamma_c \approx 15 \pm 5$ mN/m: it is highly nonpolar.

When a droplet of Na_2SO_4 ($S = 1$, $\sigma = 95$ mS/cm) solution is made to evaporate on a hydrophilic surface, the first crystals appear only when the droplet has reached a very high supersaturation of $S \approx 1.8$. The value of S is deduced by calculating the concentration in the droplet at time t when the first crystals appear. The latter is defined knowing the registered weight of the droplet at time t and the weight of salt present at time $t = 0$ in the deposited droplet of known weight m_0 and volume $V_0 = 50$ μL . The increase of the salt concentration in the droplet with time leads to the increase of the liquid surface tension γ_{lv} .¹⁶ If the contact line is not anchored on the substrate, which is the case at least for early times in the experiment, the surface tension increase is anticipated to lead to an increase of the contact angle on the basis of Young’s equation, as is seen in the experiments.¹⁹

Once a supersaturation of $S \approx 1.8$ is reached, the crystallization starts at the edge of the droplet, at the contact line of the droplet, followed by the apparition of some crystals at the liquid–air interface and the growth of dendritic patterns on the hydrophilic surface in what appears to be a precursor wetting film spreading out from the drop edge (Figure 3). The morphology of these crystals when compared with the reported crystalline shape of sodium sulfate, needles (phase III) and prismatic (phase V) structures,^{20,5} reveals the formation of the anhydrous Na_2SO_4 crystal directly from the solution. Moreover, the value of supersaturation reached before crystallization is also in good

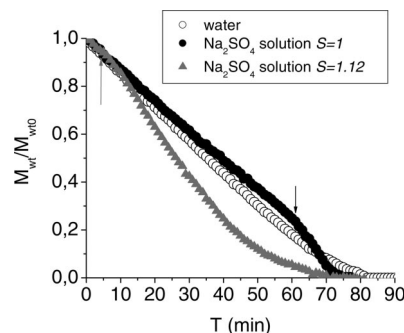


Figure 4. $M_{\text{water}}(t)/M_{\text{water}}(t_0)$ (M = mass) as a function of time during the evaporation of pure water droplets and sodium sulfate droplets for $S = 1$ ($M_{\text{salt}} = 0.0099$ g in the droplet) and $S = 1.12$ ($M_{\text{salt}} = 0.00118$ g). The mass of the salts has been subtracted from the total weight of the droplet. The gray arrow indicates the point where the drop starts to spread after the formation of hydrated crystals at the interface, and the black arrow indicates the start of observable anhydrous crystal growth at the contact line.

agreement with the value of the concentration reported for the solubility limit of thenardite (35 wt %, 21 °C) and is very large compared to the maximum mirabilite saturation (16.5 wt % at 21 °C).^{2,3}

It can be concluded that the nucleation of hydrated crystals is very difficult. The solution at 95 mS/m is in equilibrium and does not contain any mirabilite seeds compared to a solution at 108 mS/cm. During evaporation, although highly supersaturated with respect to the formation of mirabilite, the solution reaches thenardite saturation; subsequently, direct crystallization of anhydrous salt starts at the contact line. The formation of anhydrous crystals suggests that this is easier kinetically. For crystallization on a hydrophobic surface, the kinetics of evaporation and crystallization remain very similar, except for the fact

(20) Amirthalingam, V.; Karkhanavala, M. D. *Acta Crystallogr., Sect. A* **1977**, *33*, 522–552.

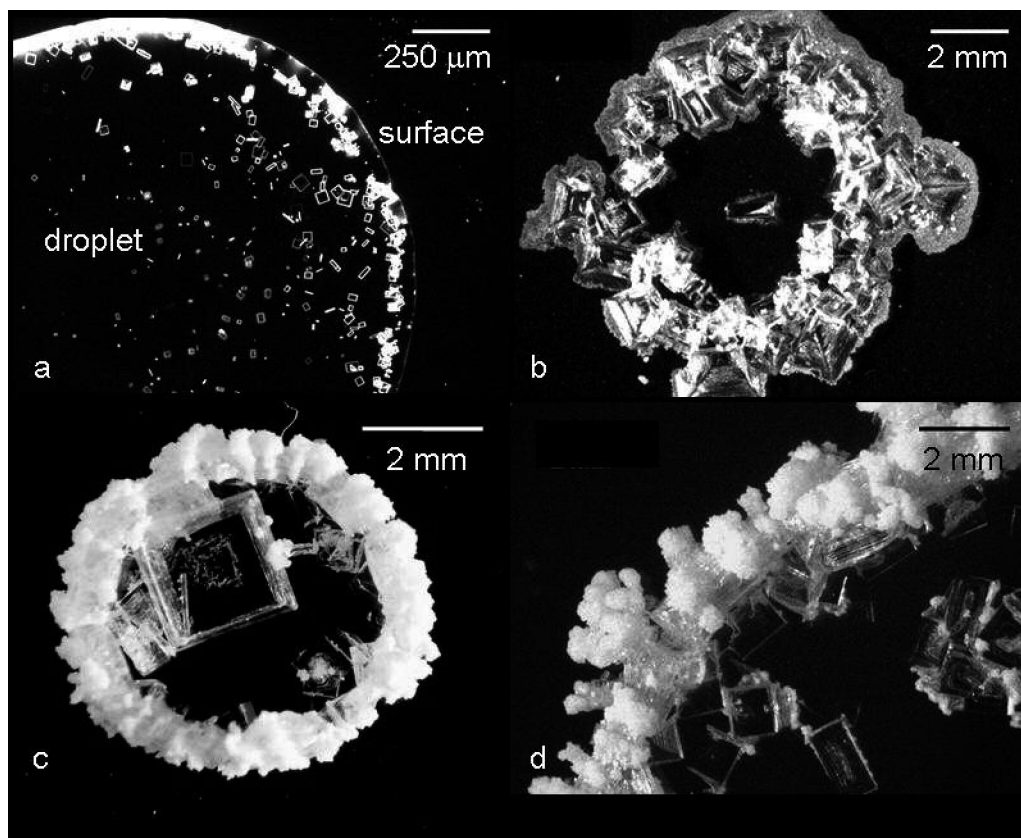


Figure 5. Crystallization during evaporation of saturated NaCl droplets. Hydrophilic surface: (a) growth of cubic crystal at the liquid–air interface, (b) ringlike crystalline deposit surrounded by a small spreading film. Hydrophobic surface: (c) crystallization pattern, (d) close-up of the cauliflower-like morphology on the border.

that, due to the absence of the wetting precursor film, the dendritic thenardite structure cannot grow onto the solid surface beyond the drop edge.

The measurement of the time evolution of the weight of evaporating droplets for both solutions ($S = 1$, $S = 1.12$) and water placed on a hydrophilic substrate is shown in Figure 4. The results show for water an almost linear behavior (constant evaporation rate); since the evaporative flux is known to be proportional to the perimeter of the droplet, a constant rate suggests a constant perimeter due to the anchoring of the droplet on the substrate. That the rate is proportional to the perimeter rather than the area has been shown by Shahidzadeh et al.²¹ and in earlier work by R. Deegan et al.²² The fundamental theoretical reason for this is that, theoretically, the evaporative flux diverges at the boundary and consequently the evaporation rate is dominated by the boundary (perimeter) term rather than the surface area.²²

For water, the evaporation rate is about 6.8×10^{-6} g/min. For a droplet of Na_2SO_4 ($S = 1$), a constant rate period of 5.8×10^{-6} g/min is observed just before the crystallization growth starts (i.e., $S \approx 1.8$). This smaller evaporation rate is due to the fact that the vapor pressure of the salt solution is lower than that of the pure water; the equilibrium RH above a saturated Na_2SO_4 solution was measured to be 93%. As soon as the anhydrous crystals start to grow (indicated on the graph with a black arrow), a film is observed to spread out from the contact line concomitant with the growth of the dendritic structures. The enlargement of

the perimeter makes the drying faster. For the supersaturated solution, the spreading of the droplet 5 min after its deposition is clearly visible on the graph (indicated with a gray arrow). The formation of the film increases the evaporation rate due to the larger perimeter, and since the spreading is very large, this is the fastest evaporation process.

The evaporation of saturated NaCl solutions on a hydrophilic surface results in the formation of small cubic crystals at the liquid–air interface (Figure 5). The growth of these crystals again decreases the liquid–vapor interfacial tension, leading to the observation of a slight spreading (its radius increases by about 10%) of the droplet. The spreading is less pronounced than for a Na_2SO_4 solution, probably because of the higher solubility of NaCl. There is a higher ion concentration and therefore a higher liquid–vapor interfacial tension at saturation: $\gamma_{\text{NaCl solution}} \approx 84$ mN/m. At the end of drying, a ringlike crystalline deposit in the border is observed (Figure 5b). This is reminiscent of the well-known “coffee-stain effect”, which is usually attributed to a capillary flow from the center to the border of the drop driven by the loss of solvent by evaporation, in combination with pinning of the contact line (the border of the drop) at defects on the surface.²² On a hydrophobic surface, contrary to what happens for the hydrophilic case, the NaCl crystallization appears not at the liquid–air interface but rather at the solid–liquid interface. At the end of the evaporation a *cauliflower-like* structure is observed to grow on top of the cubic crystals at the drop edge (Figure 5d).

From the experiments, it can then be concluded that sodium chloride crystals prefer to grow in contact with a nonpolar environment such as air or a silanized solid surface.

(21) Shahidzadeh, N.; Rafai, S.; Azouni, A.; Bonn, D. *J. Fluid Mech.* **2006**, *549*, 307–313.

(22) Deegan, R. D.; Bakajin, O.; Dupont, T. F.; Huber, G.; Nagel, S. R.; Witten, T. A. *Phys. Rev. E* **2000**, *62*, 756.

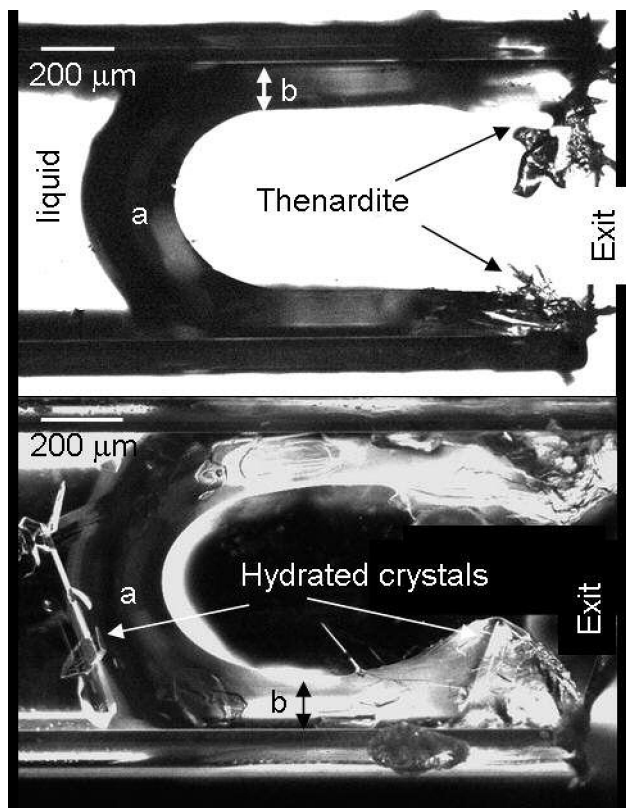


Figure 6. Crystallization during evaporation in square capillary tubes ($800 \times 800 \mu\text{m}$) of Na_2SO_4 solution ($S = 1$) (growth of thenardite at the contact line at the exit of the tube) and Na_2SO_4 solution ($S = 1.12$) [growth of hydrated crystals at the liquid–air interface of the meniscus (a) and thick wetting films in the corners (b)].

Evaporation from Capillaries. The evaporation of the salt solution droplets was followed by experiments on the evaporation of the same solutions in square capillaries. These serve as a simple model system for a single pore in a porous medium. All capillaries used are hydrophilic after being cleaned with sulfochromic acid. As already mentioned, salt crystallization in circular capillaries has been studied in some detail,^{10,23} but in angular (square) capillaries it has not. Still, one of the key features of pores in porous media is the existence of axial channels or grooves that can retain wetting liquids. Consequently, cylindrical capillaries are too simple to reveal the actual fluid retention in the irregular pore structure of real porous media such as stones. Due to capillary forces, the wetting phase has a tendency to collect in the corners of an angular capillary when a nonwetting phase such as air invades a fluid-saturated capillary tube. The difference between our experiments in square capillaries and previous works in cylindrical ones is that for the latter the thick films in the corners are not present. This greatly reduces the evaporation speed and thus drastically slows the evaporation rate. Moreover, the drop evaporation experiments have underlined the importance of wetting films on the dynamics of crystal growth on a flat surface.

Theory on ion transport in capillary tubes and porous media^{24,25} suggests that, during the evaporation, the salt distribution within the capillary depends mainly on the Peclet number, which is the ratio of the convective to diffusive transport in the liquid: $Pe =$

UL/D_{eff} , where U is the liquid average velocity, L the sample size, and D an effective diffusion coefficient. In square capillary tubes, the effect of thick liquid films in the corners will greatly increase the drying rate and hence enhance ion transport ($Pe > 1$). Therefore, the onset of crystallization is expected to occur much earlier, and the strong convective effect within the film should induce a significant salt accumulation at the tube entrance.²⁴ From these arguments, it was suggested that the crystallization would occur preferentially at the tube entrance rather than in the bulk. We therefore study experimentally the evaporation of both NaCl and Na_2SO_4 solutions in square capillaries. The $800 \times 800 \mu\text{m}$ capillaries are horizontal, and crystallization is observed directly under a microscope during evaporation.

For the Na_2SO_4 solution with a conductivity $\sigma = 95 \text{ mS/cm}$ ($S = 1$), we observe the formation of anhydrous (thenardite) crystals at the edge of the wetting film concomitant with the growth of dendritic patterns outside the tube. No crystals were found in the bulk solution (Figure 6). These results agree perfectly well with what was expected both from the droplet experiment and from theory.

On the other hand, the evaporation of a $\sigma = 108 \text{ mS/cm}$ ($S = 1.12$) solution reveals the formation of hydrated crystals at the liquid–air interface both in the thick liquid films in the corners and at the meniscus deep within the tube (Figure 6). The formation of these crystals leads again to a further spreading of the thick wetting film with time. Consequently, the liquid comes out of the tube and crystallizes on the walls outside of the capillary: this is a clear manifestation of efflorescence, observed in a single capillary. The results agree with the observation from the drop evaporation experiments but do not agree completely with the theoretical prediction.

For the NaCl -saturated solutions, cubic crystals appear at the liquid–air interface both at the meniscus and on the thick films (Figure 7). Crystals formed at the liquid–air meniscus can flow through the thick film due to the high convective transport in these films. Just as in the drop experiments, there is a slight spreading of the solution at the exit of the capillary, leading to an efflorescence crystallization growth outside of the capillary tube. The latter should again be due to the decrease of liquid surface tension with the growth of cubic crystals at the liquid–vapor interface.

Discussion and Conclusion

The question posed initially was whether there was a relation between the interfacial properties and the location of crystallization leading to the efflorescence or subflorescence for two different salts: sodium sulfate and sodium chloride.

From drop evaporation experiments it can be concluded that the wetting behavior of the crystals is of paramount importance for how the crystallization growth and pattern evolve.

Sodium chloride crystals are found to form preferentially in contact with a nonpolar area (air or hydrophobic solid). This is an important observation, since hydrophobic treatments have been used frequently in the past to prevent crystallization and damage on buildings. Our observations suggest that this may be counterproductive due to the tendency of NaCl to crystallize on nonpolar surfaces.

Hydrated sodium sulfate and anhydrous sodium chloride crystals were observed to form within the square capillary, namely, at the liquid–vapor interface of both the meniscus within the tube and in the thick wetting films in the corners. Most of these crystals can therefore remain within the “pore” at the end of

(23) Benavente, A.; García del Cura, M. A.; García-Guinea, J.; Sánchez-Moral, S.; Ordóñez, S. J. *Cryst. Growth* **2004**, *260*, 532–544.

(24) Camassel, B.; Sghaier, N.; Prat, M.; Ben Nasrallah, S. *Chem. Eng. Sci.* **2005**, *60*, 815–826.

(25) Pel, L.; Huinink, H. P.; Kopinga, K. *Appl. Phys. Lett.* **2002**, *81*, 2893–2895.

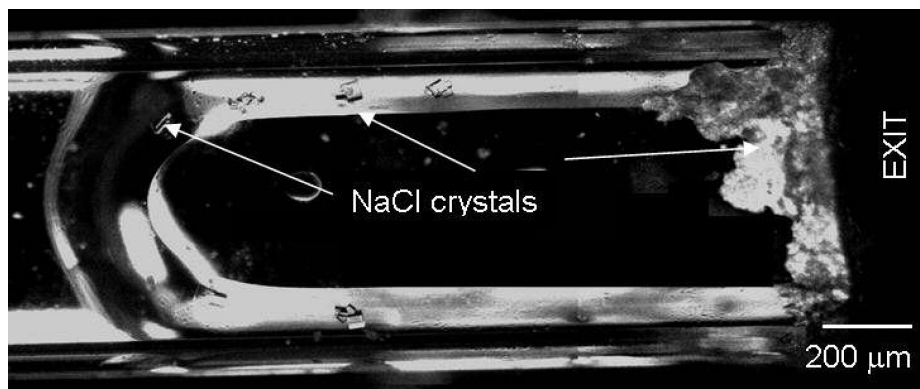


Figure 7. Crystallization during evaporation in square capillary tubes ($800 \times 800 \mu\text{m}$) of saturated NaCl solution: growth of cubic crystals at the liquid–air interface of the meniscus and thick wetting films. Efflorescence on the walls outside of the capillary tube due to the decrease of the liquid–vapor surface tension.

the evaporation, thus showing the ability of these two crystalline phases to cause subflorescence.

The formation of these crystals at the liquid–vapor interface enhances the spreading power of the solution by lowering the interfacial tension γ_{lv} during crystallization and evaporation. The enhanced spreading power leads to the wetting of the solution on the outer surface of the capillaries and consequently to efflorescence at the same time. For most practical purposes, the speed of capillary transport to the surface is larger than the evaporation rate, since the pores in real stones are usually very small. As was shown in previous works,^{26,27} the drying of porous media, in the absence of any air flow, is characterized by a constant rate period due to the liquid film and capillary rise and thus mainly limited by the amount of evaporative surface available. We have also shown that there is not necessarily a drying front during this period, which is an additional factor that could lead to subflorescence.

Anhydrous sodium sulfate crystals, which are smaller in size than the hydrated crystals, can grow directly at the contact line of the liquid films toward the exit of the tube, showing efflorescence-like behavior.

Therefore, during evaporation in square capillaries and likely in real porous media, subflorescence is observed for the hydrated crystalline phase of sodium sulfate and the cubic crystalline phase of sodium chloride. Anhydrous crystals of sodium sulfate grow directly at the contact line of the liquid films toward the exit of the capillary tube, showing efflorescence-like behavior. Anyhow, for both salts (sodium sulfate and sodium chloride), with their different crystalline phases, if the wetting films have enough time to spread toward the surface, efflorescence can be provided.

As a general conclusion, not only the transport properties in the liquid (the Pe number) but also the interfacial properties of the different crystalline phases govern the crystallization dynamics. It is the combination of these two properties that determines whether the salt solution will *effloresce* (crystallize on the outer surface of the stone) or *subfloresce* (crystallize within the stone) during evaporation, the latter being far more damaging than the former. The mechanism for the damage during drying, however, remains elusive and will be discussed in a future paper.

LA8005629

(26) Shahidzadeh-Bonn, N.; Azouni, A.; Coussot, P. *J. Phys.: Condens. Matter* **2007**, *19*, 2101–08.

(27) Coussot, P. *Eur. Phys. J. B* **2000**, *15*, 557–566.